Annals of Nuclear Medicine Vol. 6, No. 3, 123-130, 1992

3D acquisition and reconstruction in positron emission tomography

Dale L. BAILEY

MRC Cyclotron Unit, Hammersmith Hospital, London, UK, and Department of Nuclear Medicine, Royal Prince Alfred Hospital, Sydney, Australia

3D positron emission tomography (PET) refers to an acquisition geometry and reconstruction procedure that allows all coincidence events within the solid angle of the tomograph to be recorded and subsequently reconstructed. The reconstruction algorithm must consider the angle of each coincidence event relative to the central axis of the scanner. The aim of the technique is to maximise the sensitivity of the system by utilising all events that it is possible to record from the object. Conventional cylindrical 2D PET systems typically detect ~0.4%-0.5% of decaying nuclei within the field of view; with a 3D system this can increase to over 3%. Reconstruction in 3D using filtered-backprojection techniques has been developed and provides results that show little degradation of physical characteristics compared with 2D systems, apart from an increased scatter event rate. 3D techniques may be used to (i) improve data quality using currently acceptable doses of radioactivity and scanning times; (ii) extend the scanning period for short-lived tracers, especially ^{11}C-labeled ligands; or, conversely (iii) decrease injected doses of radiotracer or reduce scanning times to achieve similar results as those using current methods in 2D.

Key words: Positron Emission Tomography (PET), 3D reconstruction, instrumentation

INTRODUCTION

MODERN POSITRON EMISSION TOMOGRAPHIC (PET) scanners have intrinsic resolutions of typically around 4 mm for block-type detectors[1] and as low as 2.6 mm for specialized development systems.[2] These performance figures remain essentially hypothetical and are rarely achieved when applied to human studies when operating in the conventional mode (referred to as 2D), however, because the sensitivity of the scanners is insufficient to support reconstruction using filtered-backprojection with a high resolution (ramp) filter. One obvious way to increase the sensitivity of multiplane devices is to remove the interplane septa, which are included in the design of a tomograph to limit the acceptance of scattered and accidental (random) coincidences. This, combined with the hardware modifications to allow the acceptance of all coincidences over the full axial field-of-view increases the inherent sensitivity of the scanner with maximal gain in the axial center of the tomograph, and is referred to as full volumetric or 3D mode. Concomitant with this is the need to reconstruct the data with an algorithm that takes the angle of the event into account. The first application of such an algorithm was described only as recently as 1976.[3] Techniques now exist to extend the familiar convolution-backprojection technique[4] from two to three dimensions.[5-9]

The aim of 3D techniques in PET is to increase the sensitivity of present scanners to, firstly, improve the signal-to-noise ratio on reconstructed images and, secondly, to produce results that, in spatial resolution terms, allow the data to be reconstructed with close to the intrinsic resolution of the detectors.

3D ACQUISITION

Conventional multiplane detectors are generally amenable to modification to allow them to acquire fully 3D datasets. This is done by removing the

Presented as an invited lecture at the 31st Annual Scientific Meeting of the Japanese Society of Nuclear Medicine, Matsuyama, October 1991.

For reprints contact: Dale L. Bailey, M.D., Department of Nuclear Medicine, Royal Prince Alfred Hospital, Camperdown, NSW. 2050, Australia.

interplane septa (usually made of tungsten or lead) and altering the acquisition electronics so that not only are events within a single plane accepted as coincidences, but any two events that occur within the timing window between any one detector and a fan of opposing detectors both axially and transaxially. This has been implemented in a commercial design (Siemens/CTI-953B) consisting of 16 rings of detectors, each 6.5 mm thick axially, which is dedicated to brain studies.[10] The scanner consists of two separate circular arrays of block-type bismuth germanate (BGO) detectors,[11] each consisting of 8 rings. The scanner ring diameter is 76 cm and axial field of view 10.8 cm. In 2D mode with the septa in place, coincidence events are accepted for plane differences of up 4 (see Fig. 1) giving a total of 100 planes of response. The datasets resulting from these 100 planes of response are sorted in real-time into 31 planes (each 3.2 mm thick) orthogonal to the axis of the scanner. In this mode, the total sensitivity of the scanner to a line source in air that occupies the entire axial field of view is 5020 counts. sec.$^{-1}$ MBq^{-1} (0.5% efficiency).[12] When the septa are retracted and data acquired over the full volume (3D), the sensitivity increases to ~32000 counts. sec.$^{-1}$ MBq^{-1} (3.2% efficiency), a gain of 6.4. This increase comprises two components: firstly there is a shadowing effect of the septa (8 cm long and 1 mm thick lead in this case) on the detectors which, after removal, results in approximately an increase of ~2.5, and secondly, acquiring data over the full volume results in 256 (16×16 rings of coincidences) planes of response compared with 100 in 2D (a further gain of ~2.6). For a slightly larger whole-body scanner (Siemens/CTI-951R) with a 102 cm ring diameter the equivalent measurements yield sensitivities in 2D mode of 4400 counts. sec.$^{-1}$ MBq^{-1} (0.4% efficiency) and ~20000 counts. sec.$^{-1}$ MBq^{-1} (2.0% efficiency) in 3D, a gain of 4.5.

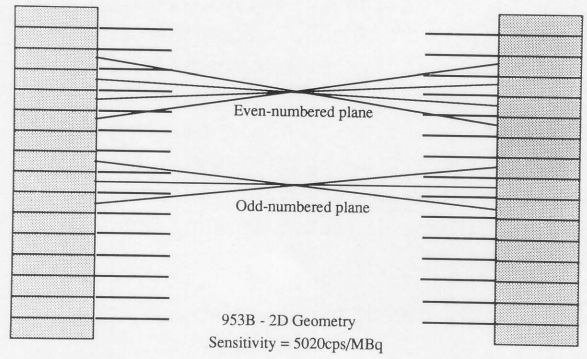

a

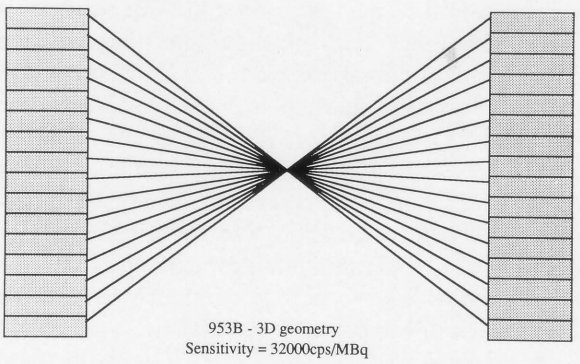

b

Fig. 1 The planes contributing to 2D and 3D datasets are shown. In the 2D case, the odd-numbered plane (planes 1, 3, 5, etc.) consists of the direct plane corresponding to the real plane (ring difference=0) plus the first two cross-planes which bisect the same mid-point (ring difference=2). The even-numbered planes in 2D are "interplanes" and consist of the immediate cross-planes (ring difference=1) plus the next pair of cross-planes which bisect the mid-point between the detector centres (ring difference=3). The 3D dataset allows any pair of rings to be in coincidence.

This gain in sensitivity must, however, be considered in the light of an increase in scatter fraction and randoms rate. The scatter fraction for a line source in a 20 cm diameter water-filled cylinder increases from 15% in 2D to over 40% in 3D. This now appears the major obstacle to implementing quantitative 3D PET, although a number of scatter correction techniques are being evaluated.[13–15] A further problem is the relatively high deadtime of block-type BGO detectors. This requires long coincidence timing windows and, hence, increases the chances of accepting a random, or accidental, coincidence. Random event rates increase as the square of the singles rates[16] and therefore, because of the much higher sensitivity of the 3D mode, amounts of activity within the field of view that in 2D mode might be considered acceptable in 3D produce very high random rates. However, the ratio of random-to-true events in 3D PET is more favorable for a given countrate compared with 2D PET.[17] This is because many single events contributing to the measurement in 2D are now accepted as valid coincidences because both photons may now be accepted, whereas before one may have been lost after interaction within the septa. Similarly for deadtime, for the same activity within the field-of-view the deadtime as a percentage will be much greater. However, many studies in 2D are count-limited and have little or no deadtime concerns, and it is in these studies that 3D techniques allow a tremendous increase in countrate without the penalty of unacceptable deadtime. Often these increases are equivalent to using 5–6 times greater amounts of radioactivity.

Real-time randoms correction using a delayed window subtraction technique[16] is implemented on

the scanners mentioned, and this increases the statistical noise in the data. Consequently, the sensitivity improvements measured must be adjusted to compensate for both the increase in scattered events and the noise due to randoms correction. This has been previously described for this scanner using the noise equivalent countrate (NEC) parameter.[17,18] Noise equivalent countrate is defined as:

$$NEC = T^2/[1+\alpha_{ci}^2)\,(T+S_i+2R_i)] \qquad (1)$$

where T=true counts, $(1+\alpha_{ci}^2)$=noise introduced by deconvolving the scatter component, Si=scatter coincidence rate and Ri=the random coincidence rate within the object. The factor of 2 is present as the scanner uses a delayed window subtraction to correct for randoms. The scanner reports (trues+scatter) as totals (T_{tot}) and therefore the following relationship has been used in practice to calculate the NEC:

$$NEC = [T_{tot}\,(T/(S+T)]^2/(T_{tot}+2fR) \qquad (2)$$

where S=scattered counts, f=the fraction of the projection subtended by the object, R=random counts and $\alpha_{ci}=0$.[18] The CTI-953B scanner used has a ring diameter of 76 cm. It has been demonstrated that, for the 3D reconstruction algorithm developed for this work, Poisson noise is propagated similarly by both 2D and 3D filtered-backprojection algorithms.[19] Therefore, as the variance has a similar form for 2D and 3D, equation (2) can be used for comparing the 2D and 3D situations, and hence calculating a gain factor for the 3D situation. The NEC gains were found to range from over sixfold at low countrate in a small object (15 cm diameter cylinder) down to near unity at high countrates in larger objects (a 20 cm diameter cylinder filled homogeneously with activity). A summary of the physical performance of the scanner is given in Table 1.

Table 1 Summary of physical performance in 2D and 3D for the Siemens/CTI-953B. The deadtime has been derived using a 2-compartment paralyzable/non-paralyzable cascaded system[25]

Parameter	2D PET	3D PET
Reconstructed Spatial Resolution (FWHM in mm ±5%)		
In air, on axis:		
Tangential	5.0	4.8
Radial	4.8	4.6
Axial	4.3	5.2
In air, +8.5 cm off-axis:		
Tangential	6.5	7.8
Radial	5.7	5.3
Axial	5.8	5.9
In scatter, on axis		
Tangential	5.6	6.3
Radial	5.0	5.5
Axial	5.0	5.4
In scatter, +8.5 cm off-axis:		
Tangential	7.3	7.0
Radial	5.3	5.9
Axial	7.1	6.4
Sensitivity in Air for a Line Source		
Absolute (ct. sec^{-1}. MBq^{-1})	5,080	32,300
Scatter Fraction (Scatter/[Scatter+Unscattered])		
In 15 cm cylinder	0.10	0.26
In 20 cm cylinder	0.16	0.41
Energy Resolution (%FWHM at 511 keV for single events only)		
In air	21%	21%
In 20 cm cylinder	23%	24%
Countrate Performance		
15 cm cylinder		
Maximum contrate (kct. sec^{-1})	248	>350
at a concentration of (kBq. cm^{-3})	366	48
for total activity in the field-of-view of (MBq)	614	81
Maximum NEC (kct. sec^{-1})	154	151
at a concentration of (kBq.cm^{-3})	259	29
for total activity in the field-of-view of (MBq)	435	48
Deadtime (μs)		
Paralyzable	1.32	2.07
Non-paralyzable	1.74	2.94
20 cm cylinder		
Maximum countrate (kct. sec^{-1})	172	280
at a concentration of (kBq.cm^{-3})	180	48
for total activity in the field-of-view of (MBq)	616	137
Maximum NEC (kct. sec^{-1})	65	50
at a concentration of (kBq.cm^{-3})	100	22
for total activity in the field-of-view of (MBq)	342	76
Deadtime (μs)		
Paralyzable	2.17	2.72
Non-paralyzable	2.81	5.54

3D RECONSTRUCTION

The 3D mode of acquisition results in a dataset containing all possible lines-of-response in a truncated cylindrical detector geometry and requires reconstruction using an algorithm that accounts for this geometry. Conventional filtered-backprojection used in 2D, where no axial component exists, has been extended to 3D with an extra filtering operation in the z-direction.[5,7] This filter has a similar effect to the ramp filter which is used to remove the blurring caused by the backprojection process in the 2D case.

A problem exists with the truncated cylindrical geometry, however; filtered-backprojection assumes a stationary point response function. It can be seen in Fig. 2 that in the 3D case not all the object is

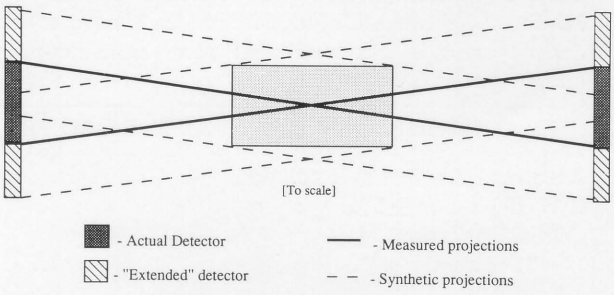

Fig. 2 The non-stationarity of the point response function in the 3D case leads to not all of the object being sampled by all projections. This can be overcome by synthetically extending the dataset based on forward projection of real measured data.

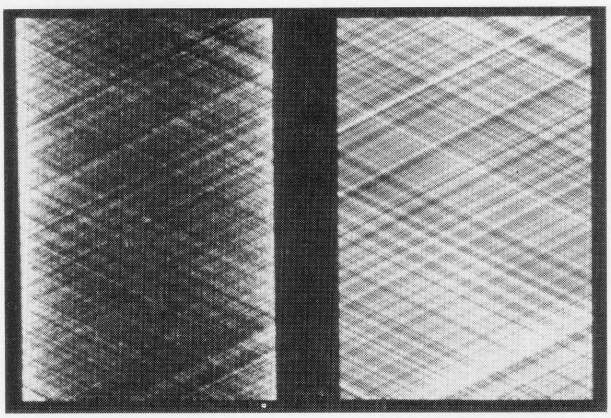

Fig. 3 Example of a plane in a 3D normalisation: (a) raw image of a single direct plane (ring 5), and (b) after processing using the method described. The variance reduction is due to the averaging of many detectors responses.

seen by all projections and this requires attention in the reconstruction procedure. One method of overcoming this is to "pad" the missing parts of the dataset to remove the axial variation of the point spread function.[6,8] This is achieved by reconstructing a subset of the data, corresponding to a conventional 2D acquisition, and forming the unmeasured lines-of-response, which correspond to angles outside the cylinder's field-of-view, by forward-projection. This results in a dataset that satisfies the stationary point spread function criteria for filtered-backprojection. The data that has been "filled in" by forward projection is relatively noiseless, compared with measured data, and in fact has the effect of improving the expected signal-to-noise ratio on the outer reconstructed planes.[9] An alternate method proposed recently, but still based on filtered-backprojection, is aimed at exploiting the oversampling, or redundancy, in some parts of the acquired 3D dataset to overcome the undersampled parts.[20] This is implemented as a modification of the filter in the z-direction, and produces results that, in signal-to-noise terms, accurately reflect the axial variation in sensitivity of the 3D mode of operation.

PRACTICAL CONSIDERATIONS AND QUANTIFICATION

Normalization

The standard technique (in 2D) for correcting for both detector sensitivity variations and geometrical effects is to acquire a high statistics scan from either rotating rod source(s) or a planar "sheet" source and measure *line-of-response* correction factors. With septa-retracted (3D) mode, these sources are often impractical because of deadtime considerations. In a separate issue, acquisition of a normalization scan that would yield a variance of $\leqq 5\%$ for each line-of-response in 3D would require the acquisition of 3Gcts in total because of the increased number of lines-of-response. This is also often impractical, as at low countrates (because of deadtime losses) this would take very many hours.

The solution that has been proposed[21] is based on the variance-reduction technique of Casey and Hoffman.[22] Using a modified version of this method, *individual detector efficiences* are determined from an ensemble of lines-of-response in a fan of coincident detectors and treated as 16 contiguous septa-extended "single-ring" studies. The mean number of counts (n) in any line-of-response (for detectors i and j), extended to the 3D geometry, is then given by:

$$\langle \boldsymbol{n}_{ij}{}^{\alpha\beta} \rangle = \varepsilon_i{}^{\alpha} \varepsilon_j{}^{\beta} \boldsymbol{g}_{i+N/2-j} \mu^{\alpha} \mu^{\beta}$$

where α and β are the rings containing the detectors i and j respectively, ε refers to the individual detector efficiency, $\boldsymbol{g}_{i+N/2-j}$ are the geometric correction factors for the fan of detectors in coincidence with detector i, and μ is the factor modifying the effective crystal efficiency due to septal shadowing, assumed to be constant within a ring. In practice a 2D "blank" scan, consisting of 16 direct planes only, containing 175–200 Mcts is acquired (usually 60 minutes) with 3 rotating rod sources (40–80 MBq per rod). The septa are extended into the field-of-view. Figure 3 shows the raw data acquired for one such direct plane (ring 5), and the resultant normalization file after processing for the same plane in the 3D dataset.

Attenuation correction

For reasons similar to those cited previously for normalization, acquisition of measured transmission data in 3D with septa retracted is impractical. As the scanner is used for both 2D and 3D acquisitions it is unrealistic to change between rod sources of different activities to suit 2D or 3D. Therefore, transmission is measured using 3 rotating rod sources of

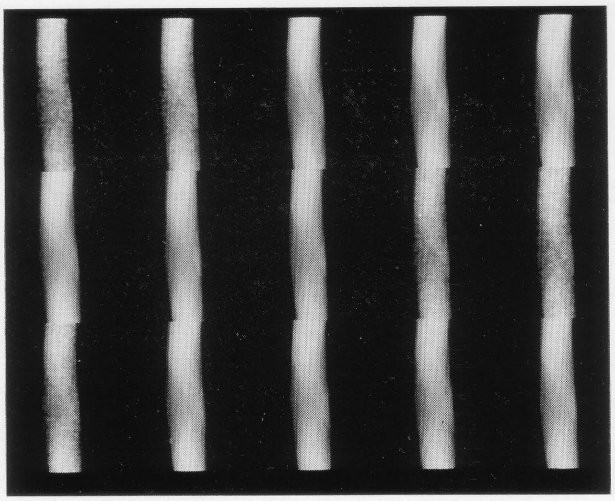

Fig. 4 Examples of real and synthetic attenuation correction sinograms for a brain study. The measured sinograms can be distinguished by the increased noise level. The synthetic sinograms, which comprise 225 of the total of 256 sinograms, are less noisy after forward projection because of the implicit integration in this procedure.

^{68}Ge in the usual 2D mode, as is a "blank" scan (transmission scan without an object in the field-of-view). The data are reconstructed and from this a full 3D set of correction factors is generated by forward projection to fill in the unmeasured angles. This is similar to the method used to remove the point-spread function variation in the emission dataset in this truncated cylindrical geometry. This results in a large number of synthetic, largely noise-free correction sinograms (Fig. 4). For studies of the brain, this approach is felt to be justified because of the relative homogeneity of attenuation, but may require further investigation for other regions of the body.

Scatter correction

Scatter increases dramatically in 3D mode compared with 2D. Comparison of a ^{68}Ge needle source unattenuated, and attenuated by a 20 cm diameter water-filled cylinder, demonstrate a scatter fraction of 16% in 2D and 41% in 3D for the CTI 953B. Interplane septa are included in the design of PET scanners to reduce scatter, especially in the axial direction, and to reduce random event rates. Therefore any scatter correction must account for scattering in this direction, which is "out-of-plane" scatter. One method is to use a dual energy window approach,[14] an idea borrowed from single photon tomography.[23] An alternative is based on the convolution-subtraction method.[24] An extension of this technique, to iteratively use successive estimates of the scatter-free distribution as the input for the convolution[15] has been implemented. The sinograms corresponding to direct plane projection data ($\theta=0°$) are reformatted to give essentially planar projections ("planagrams"), of which there are 192 ([number of detectors per ring (384)]/2) over 180°. Scatter is then estimated by convolution with a previously determined radially symmetric mono-exponential scatter function ($s=\exp(-0.10\times R)$, R in cm). This is successively updated to give a better scatter estimate via:

$$g_n=g_0-\mathrm{k}(g_{n-1}*s)$$

where g_0 is the recorded data, g_n and g_{n-1} are the the present & previous estimates of the scatter-free planagram ($g_{n-1}=g_0$ for the first iteration), k is the scatter fraction, and* indicates 2-dimensional convolution. After the scatter estimate for each planagram has been made, the scatter distributions are reformatted to give scatter sinograms for $\theta=0°$. These are subsequently subtracted from all sinograms, the non-zero θ sinograms using the scatter sinogram which bisects the z-axis of the scanner at the same point. This appears justified as, for this scanner, the maximum $\theta\leqq 7°$.

Calibration

As the sensitivity response profile is not constant in the axial direction in 3D, where it peaks in the centre of the field-of-view, a method must be adopted to remove this sensitivity effect in the reconstruction procedure. The method implemented here normalizes the integrated counts in the reconstruction to the value that would have been recorded in 2D mode *with the septa retracted.*

A calibration which is independent of scatter and attenuation is desirable: i.e., a calibration in air. This is difficult to perform in PET as the positron requires some attenuating media in which to annihilate, and this attenuates to a small degree some of the gamma photons arising from the annihilation. This has been overcome however and a calibration in air is possible.[12] A line source of aluminium containing a calibrated amount of ^{18}F is used. The thickness of aluminium is sufficient to stop all of the positrons from ^{18}F, but of course does attenuate the source to some extent. Successive sleeves of aluminium are added to the source and an attenuation curve, which is purely gamma ray attenuation, is generated. From this, extrapolation to effectively zero thickness of aluminium is possible and hence a calibration in air measurement obtained. Using this technique, which gives the absolute sensitivity of the scanner, calibration in 3D should be possible. The scanner's sensitivity to a line source in air has been determined in the 2D septa-retracted mode, and this value (in cts. sec.$^{-1}$ MBq^{-1}) can then be employed to

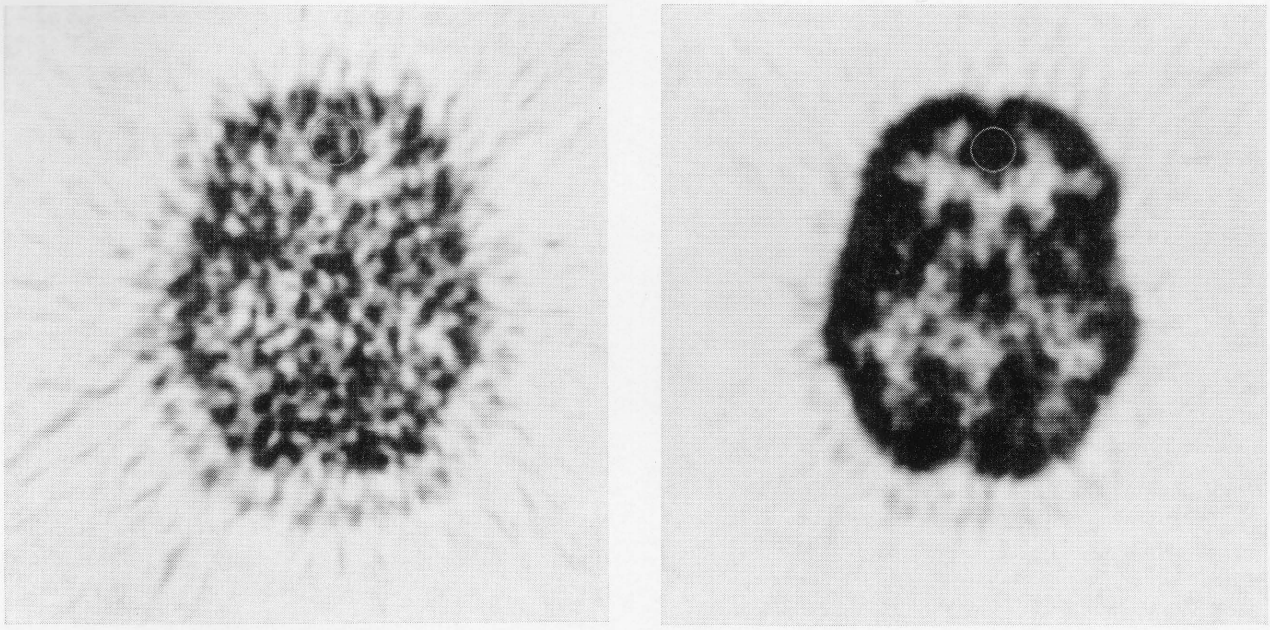

a b

Fig. 5 Example of an ^{18}F-DG study in 2D and 3D. The subject was studied one week apart under identical conditions. The gain in the 3D image compared to the 2D is approximately fivefold.

cross-calibrate against a well-counter, or convert reconstructed counts to absolute activity units using the equation:

$$\text{Activity. cc}^{-1} = \text{Reconstructed cts. s}^{-1}\text{. pixel}^{-1}\text{. plane}^{-1} \times n \text{ views} \times (\Delta/s)^2 \times (1/[\Delta^2 \times \text{plane thickness}]) \times [1/\text{absolute sensitivity factor (cts. s}^{-1}\text{. MBq}^{-1})]$$

where Δ=reconstructed pixel size, s=sampling pixel size, n views=192 for this scanner. The sensitivity value used for the CTI-953B is 12476±210 cts. sec^{-1}. MBq.$^{-1}$ This value has been measured for a scatter-free situation, and can only be used after scatter correction of the emission data.

3D ACQUISITION AND RECONSTRUCTION APPLICATION IN MAN

In the initial assessment of 3D techniques in human studies a range of labeled tracers have been examined including ^{18}F-DG, ^{18}Fluorodopa, ^{11}C-deprenyl, ^{11}C-flumazenil, ^{11}C-diprenorphine, and $H_2{}^{15}O$. Many PET studies employing ^{18}F and ^{11}C are low countrate studies in 2D, and therefore can potentially be improved greatly by using a 3D acquisition. Blood flow measurements with $H_2{}^{15}O$, especially when used as a bolus, may present deadtime problems for block detectors when using conventional doses, and strategies that optimize delivery of the tracer to maximize signal-to-noise gains require further investigation.

Noise equivalent countrate gains of approximately fivefold have been achieved using the 3D method with ^{11}C-diprenorphine.[17] This is equivalent to administering five times the activity to the subject. Not only does this provide higher quality images statistically, but also provides higher resolution reconstructions because reconstruction filters with higher frequency cut-offs may be used. A problem with many radioligand studies with ^{11}C labels is that the process being studied (for example, modeling receptor affinity or occupancy) is relatively slow with respect to the halflife of ^{11}C ($t_{1/2}$=20.4 mins). The use of 3D techniques allows the study to span a much greater sampling period than conventionally in 2D because of the increase in sensitivity. Whereas many studies previously were only possible for 40–60 mins, studies extending to up to 2 hours or more should be possible.

An example from an ^{18}F-DG study is shown in Fig. 5. Two dynamic scans were acquired 7 days apart; in the first study 152 MBq of ^{18}F-DG was administered after overnight fasting and a dynamic sequence recorded for 75 minutes (frame rates were 6×30 seconds, 7×60 seconds, 13×300 seconds) in 3D. In the second study, under identical fasting conditions, the same amount of activity was administered and the same frames acquired in a 2D sequence. The figure shows a 5 minute frame taken at 71–75 minutes for both the 2D and 3D scans. The 3D scan, which has not been corrected for scatter, demonstrates the advantage of 3D which quantita-

tively is equivalent to a fivefold increase in counts, or put another way, a 25–30 minute equivalent 2D image. This is an example of a study where high deadtime is not a major concern: the maximum (uncorrected) countrates for this study were 14 kcps in 2D and 92 kcps in 3D, both well below a level which would lead to significant count losses.

Studies of regional cerebral blood flow (rCBF), and especially activation studies where the subject is asked to perform a task, are another area of great interest where 3D studies offer potential advantages. As the radiotracer (usually $H_2{}^{15}O$ or $C^{15}O_2$) administration method is typically a bolus or short infusion this normally results in high countrates. Block-array detectors, as in the CTI scanners, are not well suited to these sorts of studies as they usually have relatively long deadtimes (see Table 1). In 3D the effects are accentuated, and the protocols for such studies in 3D need to be reconsidered. Initially, this problem has been overcome by dividing the dose into smaller amounts and performing more acquisitions up to delivering the same total dose. This obviously increases the scanning time. Given the same administered dose, however, gains of 3–4 times are expected and may permit statistically significant results for assessing change between a resting state and performance of the task in a single individual. This has not been possible previously, and 4–6 subjects were normally required to produce a single result. This is also compromised by the need to transform the different subject's brains to a common brain atlas so as to combine the data.

3D studies in areas of the body apart from the head are yet to be investigated but remain areas of great interest, especially the thorax for heart and lung studies. Potential problems here include the high countrates usually observed during the first transit of radiotracer through the heart and lungs leading to high random event rates and deadtime, the greatly increased scatter fraction that would be expected, the ability of a scatter correction regime to cope with the vastly heterogeneous density (and hence scattering properties) in the thorax, and the efficacy of generating synthetic "padded" sinograms to satisfy the stationary point spread function criteria in an area where both shape and density are varying rapidly. Interest in receptor studies in heart and lung could potentially benefit greatly from the 3D technique as they are often low countrate and ^{11}C labels. This is to be the subject of further investigation as whole-body scanners become more widely available.

CONCLUSIONS

The use of 3D techniques in PET offers a great sensitivity gain using existing technology. It also allows for higher resolution studies in human studies, not because of any inherent improvement in resolution in the 3D procedure itself, but because the higher sensitivity permits reconstruction with filters which are less compromised by noise i.e. ramp filters may be used in the pre-backprojection filtering step. The technique does suffer from an increase in scatter fraction which may account for up to 30% or more of acquired events in studies of the human brain. This may be much higher, perhaps unacceptably, in studies of the thorax or abdomen, and is yet to be investigated.

The 3D approach may be used for (i) improving data quality using currently acceptable doses of radioactivity and scanning times; (ii) extending the scanning period for short-lived tracers, especially ^{11}C-labeled ligands, for improved modeling accuracy; or, conversely (iii) decreased injected doses of radiotracer or reduced scanning times to achieve similar results as those using current methods in 2D.

ACKNOWLEDGMENTS

The work reported in this paper is the culmination of many years of toil by a large number of people. These include David Townsend and Antoine Geissbühler (*University Hospital, Geneva*), Terry Jones, Terry Spinks, Jon Heather, and Sylke Grootoonk (*MRC Cyclotron Unit, Hammersmith*), Michel Defrise (*Free University, Brussels*), Christian Michel (*Catholic University of Louvain-le-Neuve*), Ron Nutt, Mike Casey, and Larry Byars (*CTI, Knoxville*), and Maria-Carla Gilardi (*Hospital San Raffaele, Milano*). Further, we have enjoyed strong clinical support and encouragement from Richard Frackowiak, John Watson and Barry Snow (on leave from the University of British Columbia/TRIUMF) at the MRC Cyclotron Unit, Hammersmith. The author was merely fortunate to be involved in the project as it approached fruition.

REFERENCES

1. Dahlbom M, Hoffman EJ: An evaluation of a two-dimensional array detector for high resolution PET. *IEEE Trans Med Imag* 7: 264–272, 1988
2. Derenzo SE, Huesman RH, Cahoon JL, et al: A positron emission tomograph with 600 BGO crystals and 2.6 mm resolution. *IEEE Trans Nucl Sci* NS-35: 670–674, 1988
3. Orlov SS: Theory of three-dimensional reconstruction. 1. Conditions of a complete set of projections. *Sov Phys Crystallography* 20: 312–314, 1976
4. Ramachandran GN, Lakshminsrayanan AV: Three-dimensional Reconstruction from Radiographs and Electron Micrographs: Application of Convolutions instead of Fourier Transforms. *Proc Nat Acad Sci USA* 68: 2236–2240, 1971
5. Colsher JG: Fully three-dimensional Positron Emission Tomography. *Phys Med Biol* 25: 103–115, 1980

6. Townsend DW, Spinks T, Jones T, et al: Three-dimensional reconstruction of PET data from a multi-ring camera. *IEEE Trans Nucl Sci* NS-36: 1108–1112, 1989
7. Defrise M, Townsend DW, Clack R: Three-dimensional image reconstruction from complete projections. *Phys Med Biol* 34: 573–587, 1989
8. Kinahan PE, Roger JG: Analytic 3D image reconstruction using all detected events. *IEEE Trans Nucl Sci* NS-36: 964–968, 1989
9. Defrise M, Townsend DW, Geissbühler A: Implementation of three-dimensional image reconstruction for multi-ring tomographs. *Phys Med Biol* 35: 1361–1372, 1990
10. Spinks TJ, Jones T, Bailey DL, et al: Physical Performance of a new commercial positron tomograph with retractable septa. *IEEE Med Imag Conf Record* pp 1313–1317, 1991
11. Casey ME, Nutt R: A multislice two dimensional BGO detector system for PET. *IEEE Trans Nucl Sci* NS-33: 460–463, 1986
12. Bailey DL, Jones T, Spinks TJ: A Method for Measuring the Absolute Sensitivity of Positron Emission Tomographic Scanners. *Eur J Nucl Med* 18: 374–379, 1991
13. Townsend DW, Geissbühler A, Defrise M, et al: Fully Three-Dimensional Reconstruction for a PET Camera with Retractable Septa. *IEEE Trans Med Imag* 10: 505–512, 1991
14. Grootoonk S, Spinks TJ, Jones T: Correction for Scatter Using a Dual Energy Window Technique in a Tomograph Operated Without Septa. *IEEE Trans Med Imag*, 1992 (in press)
15. Bailey DL, Hutton BF, Meikle SR, et al: Iterative Scatter Correction Incorporating Attenuation Data. *Eur J Nucl Med* 15: 452, 1989
16. Hoffman EJ, Huang S-C, Phelps ME, et al: Quantitation in positron emission computed tomography: 4. Effect of accidental coincidences. *J Comput Assist Tomogr* 6: 987–999, 1981
17. Bailey DL, Jones T, Spinks TJ, et al: Noise Equivalent Count Measurements in a Neuro-PET Scanner with Retractable Septa. *IEEE Trans Med Imag* 10: 256–260, 1991
18. Strother SC, Casey ME, Hoffman EJ: Measuring PET Scanner Sensitivity: Relating Countrates to image Signal-to-Noise Ratios using Noise Equivalent Counts. *IEEE Trans Nucl Sci* NS-37: 783–788, 1990
19. Defrise M, Townsend DW, Deconinck F: Statistical noise in three-dimensional positron tomography. *Phys Med Biol* 35: 131–138, 1990
20. Defrise M, Townsend DW, Clack R: A new algorithm for 3D image reconstruction from truncated 2D parallel projections. *IEEE Trans Med Imag*, 1992 (in press)
21. Defrise M, Townsend DW, Bailey DL, et al: A normalization technique for 3D PET Data. *Phys Med Biol* 36: 939–952, 1991
22. Casey ME, Hoffman EJ: Quantitation in positron emission tomography: 7. A technique to reduce noise in accidental coincidence measurements and coincidence efficiency calibration. *J Comput Assist Tomogr* 10: 845–850, 1986
23. Jaszczak RJ, Greer KL, Floyd CE, et al: Improved quantification using compensation for scattered photons. *J Nucl Med* 25: 893–900, 1984
24. Axelsson B, Msaki P, Israelsson A: Subtraction of Compton-Scattered Photons in Single-Photon Emission Computerized Tomography. *J Nucl Med* 25: 490–494, 1984
25. Cranley K, Millar R, Bell TK: Correction for Deadtime Losses in a Gamma Camera/Data Analysis System. *Eur J Nucl Med* 5: 377–382, 1980